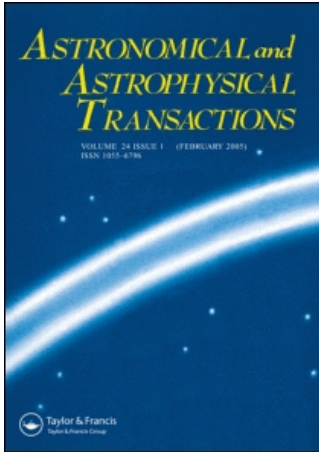


This article was downloaded by:[Bochkarev, N.]
On: 10 December 2007
Access Details: [subscription number 746126554]
Publisher: Taylor & Francis
Informa Ltd Registered in England and Wales Registered Number: 1072954
Registered office: Mortimer House, 37-41 Mortimer Street, London W1T 3JH, UK



Astronomical & Astrophysical Transactions

The Journal of the Eurasian Astronomical Society

Publication details, including instructions for authors and subscription information:
<http://www.informaworld.com/smpp/title~content=t713453505>

INTEGRAL PROPERTIES OF SOLAR ACTIVE REGIONS

O. Chumak; V. Obridko ^a; H. Zhang ^b; G. Ai ^b; V. Utrobin ^a; S. Krasotkin ^c

^a Institute of Terrestrial Magnetism, Ionosphere and Radiowave Propagation, Troitsk 142190, Russia.

^b National Astronomical Observatories, Chinese Academy of Sciences, Beijing 100012, China.

^c Scobeltsin Institute of Nuclear Physics, Moscow State University, Moscow 119899,

Russia.

Online Publication Date: 01 June 2003

To cite this Article: Chumak, O., Obridko, V., Zhang, H., Ai, G., Utrobin, V. and Krasotkin, S. (2003) 'INTEGRAL PROPERTIES OF SOLAR ACTIVE REGIONS', *Astronomical & Astrophysical Transactions*, 22:3, 335 - 355

To link to this article: DOI: 10.1080/1055679031000080366

URL: <http://dx.doi.org/10.1080/1055679031000080366>

PLEASE SCROLL DOWN FOR ARTICLE

Full terms and conditions of use: <http://www.informaworld.com/terms-and-conditions-of-access.pdf>

This article maybe used for research, teaching and private study purposes. Any substantial or systematic reproduction, re-distribution, re-selling, loan or sub-licensing, systematic supply or distribution in any form to anyone is expressly forbidden.

The publisher does not give any warranty express or implied or make any representation that the contents will be complete or accurate or up to date. The accuracy of any instructions, formulae and drug doses should be independently verified with primary sources. The publisher shall not be liable for any loss, actions, claims, proceedings, demand or costs or damages whatsoever or howsoever caused arising directly or indirectly in connection with or arising out of the use of this material.

INTEGRAL PROPERTIES OF SOLAR ACTIVE REGIONS

O. CHUMAK^{*,a,b}, V. OBRIDKO^c, H. ZHANG^a, G. AI^a, V. UTROBIN^c, and
S. KRASOTKIN^d

^a*National Astronomical Observatories, Chinese Academy of Sciences, Beijing 100012, China;*

^b*Sternberg Astronomical Institute, Moscow State University, Moscow 119992, Russia;*

^c*Institute of Terrestrial Magnetism, Ionosphere and Radiowave Propagation, Troitsk 142190, Russia;*

^d*Scobeltsin Institute of Nuclear Physics, Moscow State University, Moscow 119899, Russia*

(Received January 16, 2002)

In the paper the results of investigations on ten solar active regions are presented. The main results are as follows: firstly, the total down-flow velocity exceeds the up-flow velocity by about two orders of magnitude in all the active regions; secondly, no correlation was found between the mean integral velocity flux and the mean integral magnetic flux for all the active regions; thirdly, it was found that, besides a direct correlation between the total sunspot area and the total magnetic flux in active regions, occasionally there is an inverse correlation between these parameters, and the inverse correlation times often corresponded to the structural and topological rebuilding of magnetic flux in the active regions; fourthly, a good correlation was found between some parameters of integral fluxes (magnetic and velocity) and X-ray flux variations.

Keywords: Solar activity, solar active regions, X-ray fluxes

1 INTRODUCTION

The main idea of this investigation is to construct a few physical substantial integral state variables (SVs) for a solar active region (AR), which could be determined from observation data and allows us to define the current physical state of an AR region in real time quantitatively and uniquely. This problem has important practical meaning as such parameters can allow us to present all essential information about the current states of ARs in compact and quantitative form in order to achieve quantitative monitoring of them. Together with geomagnetic, meteorological and global solar indices, the SVs can be used as a part of the solar–terrestrial database. Such a database provides the possibility of applying modern time series analysis methods to designing geophysical and solar activity forecasts on short and medium time scales. Artificial intelligence technology (see for example the books by Murray (1995), Bishop (1995) and others) is very helpful for this purpose in our opinion, as this technology provides high-quality real-time geophysical forecasts for a short-time series.

* Corresponding author. E-mail: chumak@sai.msu.ru

The problem also has theoretical importance because statistical analysis of the quantitative parameters with clear physical meaning allows us to reveal some empirical rules, which describe a solar AR as a whole. Such empirical rules can be useful for providing a physical theory of ARs as non-equilibrium magnetoplasma structures arising and present in higher levels in the Sun and stars.

We have constructed here numerous time series of SVs. Each of these SVs has a clear physical sense and represents some property of an AR as a system in its current state. The time series analysis allows us to investigate the time variations in the state parameters of these ARs. Further, on the basis of the simple quantitative identification of the current status of ARs, the problems of the classification of ARs are discussed. As shown below, this problem has great importance for establishing the correspondence between the current physical status of an AR and its flare activity. In connection with this problem, some features of the variations in the magnetic and velocity fields before flares, during flares and after flares are discussed.

The main focus of this paper is the determination of the SVs of ARs and consideration of their time variations and cross-correlations. It is the principal feature of this investigation. All the local and fast changes in an AR are considered in close connection with its current physical state. We determine here the current physical state of an AR as a current combination of the values of the SVs.

Such a statement of the problem is the main idea of this investigation; namely the examination of solar ARs as open physical systems. At the same time this point of view corresponds to regarding a solar AR as an individual star. So such an approach makes it possible to compare some observational results for solar ARs with some corresponding results for stars, if the active processes in these stars have similar natures.

2 THE OBSERVATIONAL DATA

This investigation is based mainly on the magnetometric and Doppler observational data for the ten solar ARs obtained in 1989 at the Huairou Solar Observatory Station (HSOS) of the National Astronomical Observatory, Chinese Academy of Sciences. These data were received with a hardware-assisted solar video magnetograph. This instrument is used to receive regular data of the magnetic and velocity fields of ARs. Regular observations on this instrument are made using the Fe I ($\lambda = 5324.19 \text{ \AA}$) and H β ($\lambda = 4861.34 \text{ \AA}$) spectral lines. The device is similar to that at the Big Bear Solar Observatory (Wang *et al.* 1998). All information about the device can be obtained from the Internet site <http://bao.ac.cn>. We mention here only some features of the device. It is necessary to change the angular measurement units into linear measures.

One frame (the telescope field of vision in the charge-coupled devices (CCD) plane projection) corresponds to $4' \times 5'$ (more exactly, 3.63×5.23). It allows us to observe most of solar ARs not only partly but also as a whole in the frame. As the CCD consist of 512×512 pixels, therefore a CCD pixel corresponds to $0.425'' \times 0.613''$ or $1.373 \times 10^{11} \text{ m}^2 = 1.373 \times 10^5 \text{ km}^2 = 0.046$ million parts of Solar hemisphere (MPHs) if observations are made near the centre of the Sun's disc. For computing convenience we gathered into 12 neighbouring pixels into one discrete area. Each discrete area corresponded to the middle value of the observed physical quantity. Every frame consists of $(512 \div 3) \times (512 \div 4) = 171 \times 128 = 21\,888$ such discrete areas. The area on the Sun corresponding to a frame is equal to approximately $3.6 \times 10^{16} \text{ m}^2$ or about 12 000 mph.

TABLE I Summary data.

<i>N</i>	Number of ARs		Dates of observation		Number of H files	Number of V files	Carrington coordinates		Comment
	HSOS	NOAA ^a	Start	End					
1	36	5354	6 February 1989	15 February 1989	25	38	31.7	284.3	
2	65	5395	7 March 1989	16 March 1989	49	81	38.3	252.5	Second pass, <i>N</i> = 36
3	83	5441	7 April 1989	15 April 1989	25	38	35.5	232.6	Third pass, <i>N</i> = 36
4	192	5629	7 August 1989	16 August 1989	18		-17.5	74.3	
5	199	5634	7 August 1989	17 August 1989	25		-14.0	42.5	
6	202	5643	13 August 1989	22 August 1989	53		15.8	327.5	
7	220	5669	1 September 1989	13 September 1989	58	33	-15.8	90.5	
8	225	5680	7 September 1989	13 September 1989	88	23	15.2	2.5	
9	226	5686	8 September 1989	19 September 1989	10	4	11.8	340.2	
10	258	5747	17 October 1989	23 October 1989	37	67	-26.0	213.5	

^aNOAA, National Oceanic and Atmospheric Administration.

The time resolution of the data used in this paper does not exceed 1 min. Measurement precision is equal to ± 10 G for longitudinal magnetic field and to ± 15 G for the transverse magnetic field. The measurement precision for the velocity field is equal to ± 5 m/s⁻¹.

For this paper, about 670 magnetic and velocity maps which were obtained mainly under excellent and good visibility were selected. The maps with satisfactory visibility were added only where necessary and consisted of not more than 5–7% of the total number. All data are distributed very irregularly with respect to time and the ARs. This led to difficulties when analysing the time variations in the parameters and when comparing the results for various ARs. More detailed information about the observational data used is given in the summary data in Table I, which includes only radial velocity maps and longitudinal magnetic field maps. The total number of such maps is 545. The first column contains the numbers *N* of ARs. The second and third columns contain number of ARs obtained by the HSOS and by NOAA respectively. The fourth and fifth columns gives the dates of the start and the end of the AR observations. The sixth and seventh columns include the numbers of the magnetic field data files and velocity files respectively. The eighth column gives the Carrington coordinates of the ARs. The last column contains some comments.

3 STATE VARIABLES FOR SOLAR ACTIVE REGIONS

The method for investigating current physical conditions in local parts of the upper layers of the Sun by using integral SVs was proposed by Chumak and Chumak (1987) and then was developed by Chumak (1992). In addition to the SVs proposed in the above-cited papers we introduce here some new SVs. So it is hoped that they are sufficient (Gilmore, 1981) for a quantitative description of the non-steady processes in local regions of the solar photosphere. The definitions, computing algorithms, physical meanings and dimensions of all these integral SVs are discussed below.

3.1 Areas

The first six of these variables, namely N_{h_s} , N_{h_n} , N_{h_a} , N_{v_b} , N_{v_r} , and N_v , have the following simple geometrical meanings: N_{h_s} , number of discrete areas (*N*) with magnetic field $h > 10$ G of south polarity; N_{h_n} , number of discrete area (*N*) with magnetic field $h > 10$ G of north polarity; N_{h_a} , discrete number of both polarities with $|h| > 10$ G (so, $N_{h_n} + N_{h_s} = N_{h_a}$).

The parameters N_{v_b} , N_{v_r} , and N_v have similar meanings for the velocity (v) field. N_{v_r} corresponds to the red shift (i.e. sinking or downward movement), and N_{v_b} corresponds to the blue shift (i.e. rising or upward movement). The ‘noise level’ was taken to be equal to ± 10 G for the magnetic field and to ± 10 m s⁻¹ for the velocity field. These levels were taken to determine local AR fields from global fields, as the latter have values within these limits. So, if we multiply the values of these parameters in the one discrete area in absolute units, we obtain the whole area of corresponding features in an AR, that is area of south polarity, the area of the north polarity and so on, in absolute units.

It is evident that the ‘magnetic fields determined’ areas and ‘velocity fields determined’ areas can differ for the same AR. It is important to find out whether there is any interdependence between these state parameters or not. What is a typical variation scale of these parameters during the life of ARs? Are there any correlations between the time change in these parameters and short-time-scale active processes in ARs or not? Answers to these questions are interesting from a theoretical point of view and we shall discuss them later. Note also that the values of each of these parameters cannot exceed the value 21 888, the number of discrete values in a frame.

3.2 Fluxes

The next six parameters, H_s , H_n , H_a , V_b , V_r and V_a , also have clear physical meanings. H_s and H_n are the total flows of the longitudinal (along the line of sight) vector component of the magnetic field for N_{h_s} and N_{h_n} respectively. If we make the simple assumption that the magnetic field vectors in ARs have mainly a radial distribution, then, from a statistical-average viewpoint, the modulus of the magnetic field vector is rather more than the modulus of its longitudinal components. So low estimations of the magnetic fluxes are those used below. As the discrete area is equal to about 2×10^{16} cm² $\approx 2 \times 10^{12}$ m², then the magnetic flux for one discrete area is equal to about $H \times 2 \times 10^8$ Wb, where H is the value of the magnetic field in gauss. We omit these constants below and give values of the magnetic fluxes in relative units. To convert these into absolute units we must multiply the afore-mentioned relative units by constants. H_a is defined as a sum of the modulus of H_s and H_n : $H_a = |H_s| + |H_n|$.

The parameters V_b and V_r for the velocity field are defined in a similar way, and V_a is also given by $V_a = |V_b| + |V_r|$. The difference consists in the value and dimension of the constant for converting the relative units of hydrodynamic flow into absolute units. If we take the photosphere density (the level where the optical thickness in the H_β line is equal to 1) as about 2×10^{-4} kg m⁻³ (Allen, 1973), then for the conversion constant we have a value equal to approximately 4×10^8 kg s⁻¹, where V is the longitudinal velocity in metres per second. So to obtain hydrodynamic flow values in absolute units it is necessary to multiply V_b , V_r and V_a by this constant. It should be noted also that such hydrodynamic flow values give only a rough estimation of the order of magnitude for these values.

Is there any interdependence between these SVs or not? What is a typical variation scale of these parameters during the life of ARs? Are there any correlations between the time change in these SVs and the short time scale of physical processes in ARs or not? These are the same questions that were asked above for the first six parameters, but answers to these questions in this case are more interesting and more important as they can be easily linked to current theoretical ideas about solar plasma under photosphere dynamics and physical models of the generation of strong local magnetic fields in the upper layers of the Sun.

3.3 Energies

The following six parameters were determined for energy estimations: E_{h_s} , E_{h_n} , E_{h_a} , E_{v_b} , E_{v_r} and E_{v_a} . Energy, as is well known, is an extensive variable. So it is defined as a sum over the

corresponding numbers (N_{h_s} , N_{h_n} , etc.) of squared moduli of the longitudinal components of the magnetic field. For example E_{h_s} is a sum (of the discrete values of the south polarity) of squared moduli of the longitudinal components of the magnetic field. The other parameters of this group were computed similarly. It is clear that $E_{h_a} = E_{h_s} + E_{h_n}$, and $E_{v_a} = E_{v_b} + E_{v_r}$.

The physical meanings of this group of parameters are clear. The first three parameters (the E_h parameters) allow us to obtain the estimations of the magnetic field energy in a layer of unit thickness with equal areas for the south polarity area, for the north polarity area and for all AR areas. The second three parameters (the E_v parameters) allow us to obtain the estimations of the energy of the hydrodynamic motion in the layer of unit thickness for the red-shift area, the blue-shift area and all AR areas. The values of all parameters in this group are represented below in relative units. To convert these values into absolute values we must multiply all h parameters by a constant which is equal to approximately 2.4×10^{15} erg and all v parameters by a constant equal to approximately 2.1×10^{15} erg. As one can see, these constants have very close values and this allows us make a quantitative comparison between the energy of the magnetic fields and the energy of hydrodynamic motions in relative units.

We should make some remarks about such energy estimations that seem to be important. The kernel of the problem is in the essential dependence of these parameter values on the discrete area (area that the cell covers). This is because the dimensions of these cells determine the scale of averaging of the magnetic and hydrodynamic fields. So in this paper a cell dimension equal to approximately $1.7'' \times 1.84''$ or about $1.65 \times 10^6 \text{ km}^2$ neutralizes all magnetic and hydrodynamic flows with cross-sections less than these dimensions. We do not know the energy distributions of flows of various cross-sections and, if on a small scale the flows have considerable energy (which is quite possible), then we can underestimate the energy values. Otherwise it must be remembered that the lower values of the energy parameters cited here represent their lower bounds.

However usually there is no need to know the total energy values. It is often important to know the dynamics of their changes and in these cases our energy parameters can be very useful. So the sum $F = E_{h_a} + E_{v_a}$ gives us an estimate of the free energy of an AR. The change in F relative to the change in area gives (see for instance the book by Landau and Lifshits (1976) an estimate of the equivalent pressure in an AR. Therefore it appears possible to develop thermodynamic models of ARs, which are based on only the observational data. Such empirical phenomenology could become the starting point for the theory of ARs as dissipative structures arising and existing in the thermodynamically non-equilibrium plasma of the upper layers of the Sun. For realization of this idea it is important to be in a position to derive from observations more such parameters (the more the better) with clear thermodynamic meaning.

3.4 Entropies

In this connection let us consider the following group of parameters: S_{h_s} , S_{h_n} , S_{h_a} , S_{v_b} , S_{v_r} and S_{v_a} . These are the Shannon structural entropy parameters defined for the magnetic and velocity fields of the ARs. The values of these parameters can be easily obtained from observations in the following way. Let, for instance, h_s be the value of the longitudinal component of the magnetic field with a discrete south polarity. The ratio $p(i) = h_s(i)/H_s$ can be interpreted as the probability density of distributions of the elementary fluxes in discrete areas. Then the value of entropy of south polarity can be computed from (Klimontovich, 1987)

$$S_{h_s} = \sum_{i=1}^{N_{h_s}} p(i) \ln \left(\frac{1}{p(i)} \right).$$

All six parameters of this group were computed by similar formulae.

The range of variation in entropy values depends on the number of discrete areas over which we obtain the sum. So, if all flux is concentrated in one discrete area, then the entropy of such a flux distribution is equal to zero. If, in another singular case, H_s is uniformly distributed over all corresponding discrete areas, then the entropy reaches its maximum value equal to $\ln(N)$, where N is the number of discrete areas over which we obtain the sum. In all real cases the value of entropy lies between these two bounds. So this group of parameters can be useful as quantitative characteristics of the degree of flux concentration.

As in the case with energies, the direction (sign) and rate of time variations in these parameters are more important than its absolute values, which, as was noted above, depend on the cell dimensions. From the time series of these parameters we can estimate at any instant in time the entropy production in every polarity and in the AR as a whole to obtain their differences dS/dt . It is clear that, if $dS/dt < 0$, then an increase in the field concentration takes place at a rate $dS/dt > 0$, then the AR exhibits a relaxation tendency to smooth its fields concentration.

3.5 Coordinates

The next group of parameters uses the information on coordinates. Time variations in these parameters allow us to obtain quantitative information about the main kinematic tendencies in ARs and even to make some classification of ARs by their kinematic properties. These parameters are as follows: X_{h_s} and Y_{h_s} are the average coordinates of the south polarity centre weighted by the magnetic fluxes; X_{v_b} and Y_{v_b} are the coordinates of the blue-shift area centre weighted by the velocity fluxes; X_{h_n} and Y_{h_n} , X_{v_r} and Y_{v_r} are the north magnetic polarity and the red-shift area corresponding coordinates centres respectively; X_{h_a} , Y_{h_a} , X_{v_a} and Y_{v_a} are the average coordinates weighted by the modulus of the magnetic fluxes ‘magnetic centre’ and by the modulus of the velocity fluxes ‘velocity centre’ of an AR respectively.

In this paper all these coordinates were computed as relative and delineated by discrete numbers from the top left corner of the frames. There is no need to consider the corresponding absolute solar coordinates in this paper although observational data allow us to obtain these. So the last four parameters cannot be used for analysis of the centre of gravity of an AR. They are used here only to calculate the motions of the polarity centres relative to the centre of the AR. From these parameters we calculate the distance between the weighting centres of fluxes, R_{s_n} and R_{b_r} , and the angles between these axes and the local parallel, A_{s_n} and A_{b_r} .

We calculated also the length of field inversion lines: L_h for the magnetic field and L_v for the velocity field. Along both of these lines we summed normal to the field gradients G_h and G_v and calculated their line densities from $d_{G_h} = G_h/L_h$ and $d_{G_v} = G_v/L_v$. The last six parameters give us some additional quantitative information on the structure features of ARs.

3.6 General comments

The parameters in Sections 3.1–3.5 are the basic parameters required. Below, in the paper, other parameters appear which were calculated from these basic parameters. They will be determined as they appear in the text.

4 SOME INTEGRAL PROPERTIES OF MAGNETIC FIELDS AND VELOCITY FIELDS IN SOLAR ACTIVE REGIONS

In this section we shall discuss the most common properties of solar ARs in terms of the average values of several of their parameters. The average (over the total observation time)

values of parameters for each of the ARs were calculated from the observational data described above. We also use daily average values of the sunspots areas of the ARs and the flare indices according to *Solar Geophysical Data*, 1989, Apr. P2, May P2, Jun. P2, Oct. P2, Nov. P2, Dec. P2.

In Figure 1 we can see average (over the total observation time) fluxes in the longitudinal velocity component for six ARs. From the ten ARs considered, we obtain only six of them because for the other four (see Table 1) we had no data velocity. The open rectangles pointing down from zero correspond to downward flow (red shift, V_r) fluxes, and the full rectangles pointing up from zero the upward flow (blue shift V_b) fluxes. The numbers of ARs according to NOAA are shown along the abscissa axis. Values of the hydrodynamic flows are represented in Figure 12 in relative units. In order to obtain the estimate of the flow values in absolute units (kilograms per second) one should multiply the ordinate values by a factor of about 4×10^{14} . From this figure we can see that (for the H_β level) the downward flow fluxes are a few orders of magnitude greater than the upward flow fluxes for all the ARs. The mean square deviation for these values has the same order of magnitude as the values of the upward flow fluxes.

The ‘disbalance’ D_v between the downward flow and upward flow for every AR was calculated from the formula

$$D_v = \frac{V_b + V_r}{|V_b| + |V_r|}.$$

Taking into account that V_r is negative by definition we conclude that D_v can possess a value in the interval between +1 and -1. The value +1 corresponds to the case when one can observe upward flow only, and the value -1 when one can observe downward flow only. The case when $D_v = 0$ corresponds to exact balance of upward and downward flows.

For the six ARs shown in Figure 1, the mean observation of this parameter is equal to -0.8. The minimum value $D_v = -0.4357$ has a superactive region NOAA 5395 (March 7-17, 1989) and the maximum value $D_v = -0.997$ also has a region that is very active, NOAA 6569 (September 1-12, 1989). Some other ‘disbalance’ parameters were calculated in a similar way. Among these are the magnetic flux ‘disbalance’ D_h and the entropy ‘disbalances’ D_{s_v} and D_{s_h} due to the velocity flows and magnetic fluxes respectively. All these ‘disbalances’ parameters are important as they allow us to obtain numerical estimates of

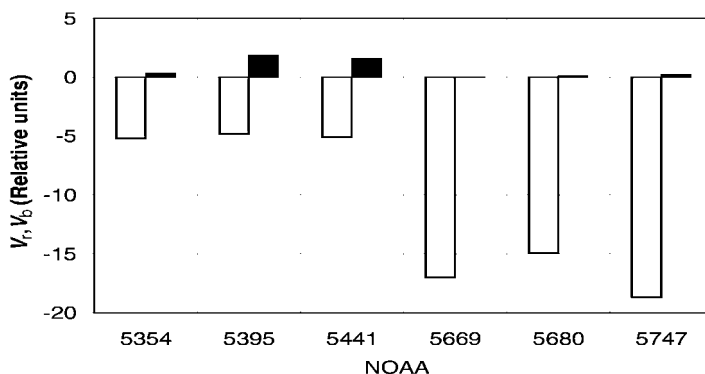


FIGURE 1 Average (over the total observation time) hydrodynamic fluxes in six ARs (in relative units): □, V_r ; ■, V_b .

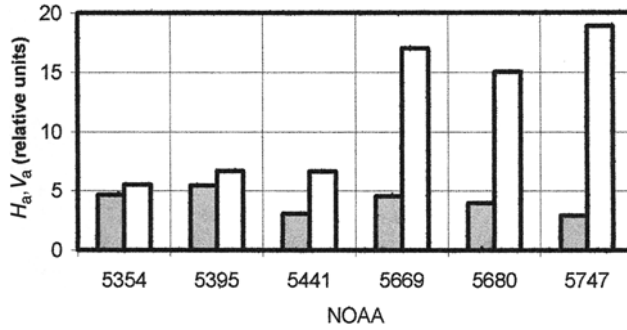


FIGURE 2 Comparison between the magnetic and the hydrodynamic fluxes: \blacksquare , H_a ; \square , V_a .

the degree of openness of the AR as a physical system. In this sense they are similar to the Trieste numbers, which were proposed by Veselovsky (1999) for a scaling description of the heliospheric plasma.

Figure 2 shows the average (over the total observation time) total hydrodynamic (V_a) and total magnetic (H_a) fluxes for each of six ARs in comparable units. Values of the hydrodynamic and magnetic flows are represented on Figure 2 in a similar way to Figure 1 in relative units. In order to obtain the estimate of the flow values in absolute units, one should multiply the ordinate values by a factor of about $4 \times 10^{14} \text{ kg s}^{-1}$ for hydrodynamic flows and by factor of about $2 \times 10^8 \text{ Wb}$ for magnetic flows. One can see a total lack of any correlation between these parameters. This fact (in particular) testifies against any connection between the magnetic field sources and the plasma motions on a photospheric level.

Figure 3 shows the average (over the total observation time) Shannon entropies of the velocity fields for the same six ARs. From this figure one can see that structure of the downward flow S_{v_r} is more complicated and smooth than that of the upward flow S_{v_b} . There is also the interesting fact that the average entropies of the downward flow plasma are almost equal to each other independently of both the total sunspot areas S and the total flare indices F of the ARs (Figure 4). The entropy ‘disbalance’ D_{S_v} for velocity field is equal to 0.23 ± 0.07 .

Figure 4 represents the average (over the total observation time) total sunspot areas S and the average relative flare indices F for seven ARs in dimensionless units: the sunspots areas S in MPHs were divided by M_S (the average S value for the seven ARs) and the relative flare indices were divided by M_F (the average F value of the seven ARs). One can see a good correlation between these parameters.

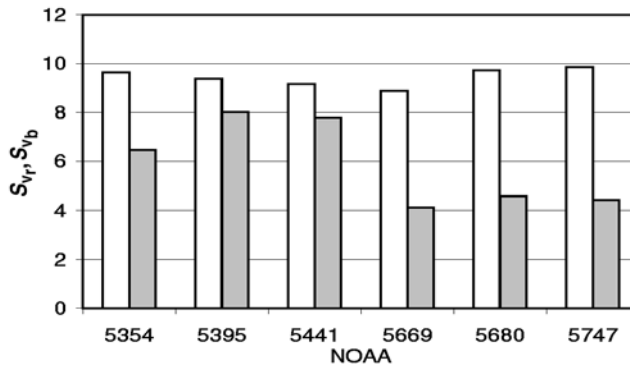


FIGURE 3 Shannon entropies of the velocity fields: \square , S_{v_r} ; \blacksquare , S_{v_b} .

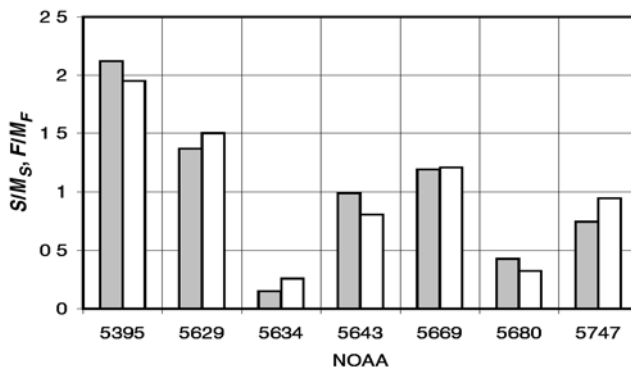


FIGURE 4 Relative total average sunspot areas S/M_S (■) and relative average flare indices F/M_F (□) for seven ARs.

Figure 5 represents the average (over the total observation time) values of magnetic fluxes for north and south polarities in all ten ARs in dimensionless units in a similar way to Figure 4. M_{H_a} is the average of the distribution of H_a . From this figure we can see that these fluxes are more balanced than plasma flows (see Figure 1). The average (over all ten ARs) ‘disbalance’ value D_h for magnetic fluxes is equal to $+0.15$ with a standard deviation of ± 0.18 . For plasma flows the ‘disbalance’ value D_v is equal to -0.80 with a standard deviation of ± 0.20 . Both the maximum value $D_h = +0.75$ and the minimum value $D_h = +0.014$ of the magnetic flux ‘disbalance’ were found to be in the regions that are least active (of the ten regions): NO 5441 and NO 5686 respectively. Figure 6 represents the average (over the total observation time) Shannon entropies of north and south magnetic fluxes for all ten ARs. We can see that the average values of this parameter for all ten regions do not have significant differences and the ‘disbalance’ of fluxes is also very small. In contrast, in the case of the velocity fields it should be recalled that a very different picture was encountered.

5 RELATIONSHIP BETWEEN THE TOTAL SUNSPOT AREAS AND THE TOTAL MAGNETIC FLUXES IN SOLAR ACTIVE REGIONS

In this section we discuss some features of the time behaviour of the total magnetic flux H_a and the total sunspot area S_a for four solar ARs (NOAA 5395, 5629, 5643 and 5680). In

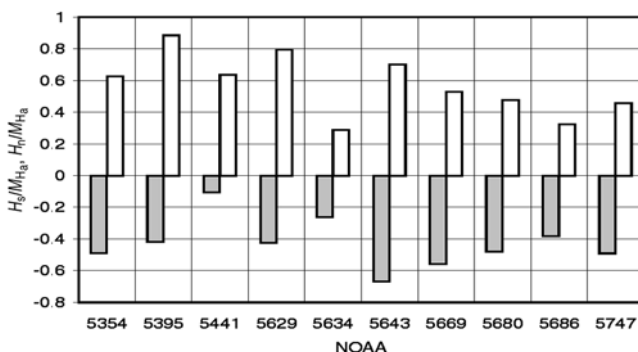


FIGURE 5 Average values of magnetic fluxes for north (H_n/M_{H_a}) (■) and south (H_s/M_{H_a}) (□) polarities in ten ARs.

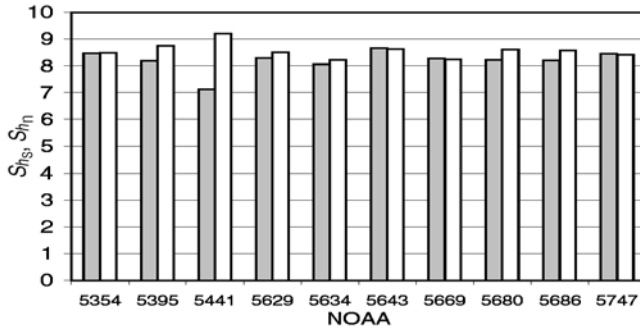


FIGURE 6 Entropies of magnetic fluxes of north and south polarities: \blacksquare , S_{H_n} ; \square , S_{H_s} .

Figures 7–10 the total magnetic flux and the total sunspot area are presented in dimensionless units: S_a/M_{S_a} and H_a/M_{H_a} , where M_{S_a} and M_{H_a} are the averages (over the total observation time) of S_a and H_a for the corresponding AR. Figures 7–10 are representative examples of time variations in the total relative (i.e. normalization by the observation time average) sunspot areas and total relative (in the same sense) magnetic fluxes for four ARs. One can see from these plots the correlations between these two parameters, from a high positive (normal) correlation (Figure 10) to a high negative correlation (Figure 7). Between these two extreme

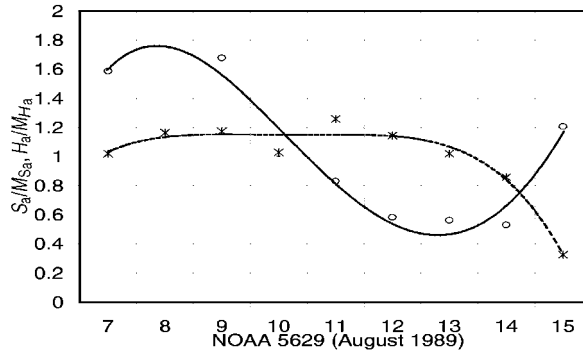


FIGURE 7 Time variations in the total sunspot area (S_a/M_{S_a}) (\times) and the total magnetic flux (H_a/M_{H_a}) (\circ) for NOAA 5629.

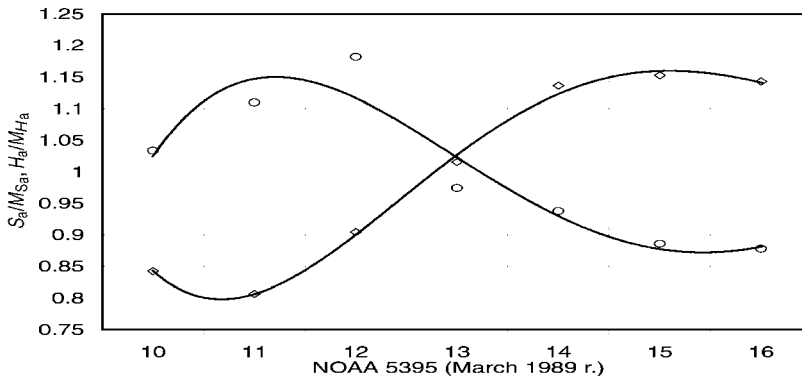


FIGURE 8 Similar to Figure 7: \circ , H_a/M_{H_a} ; \diamond , S_a/M_{S_a} .

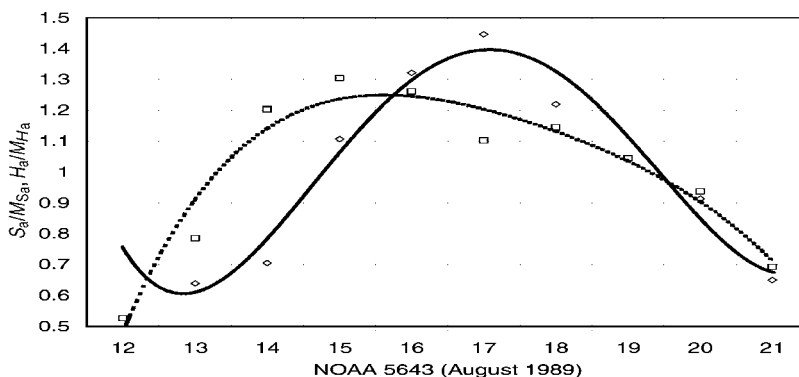


FIGURE 9 Similar to Figure 7: \diamond , H_a/M_{H_a} ; \square , S_a/M_{S_a} .

cases, one can see the shifts in the curves from each other. The ARs with positive correlations between the total sunspot area and the total magnetic flux showed low and moderate flare activity while the ARs with anticorrelations showed high flare activity. So from Figure 7 we can see that for March 10–11, 1989, a high increase in magnetic flux has occurred at the same time as minimization of the total sunspot areas. The decrease in the magnetic flux during March 12–14, 1989 coincided with an increase in sunspot area. Thus, on these dates, flares were observed in this AR.

6 TIME VARIATIONS OF DAILY AVERAGE INTEGRAL PARAMETERS

Besides the total sunspot area and the total magnetic flux there are some other integral parameters in ARs with interesting features in their time variations. As in the previous section we use here only the daily averages of the parameters.

Simultaneous time variations in the total magnetic flux in the north polarity, H_n , and its area, N_{h_n} , are shown in the Figure 11. Similar to the variables in the previous section the area and flux are given in dimensionless units. This is presented as a typical case. In particular, one can see a sharp increase in magnetic flux under a simultaneous decrease in its area during September 3–4, 1989. The case is similar to the situation on March 10–11,

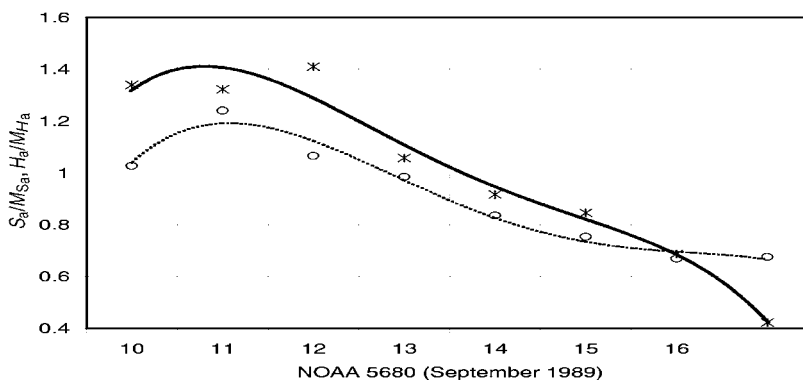


FIGURE 10 Similar to Figure 7: \circ , H_a/M_{H_a} ; $*$, S_a/M_{S_a} .

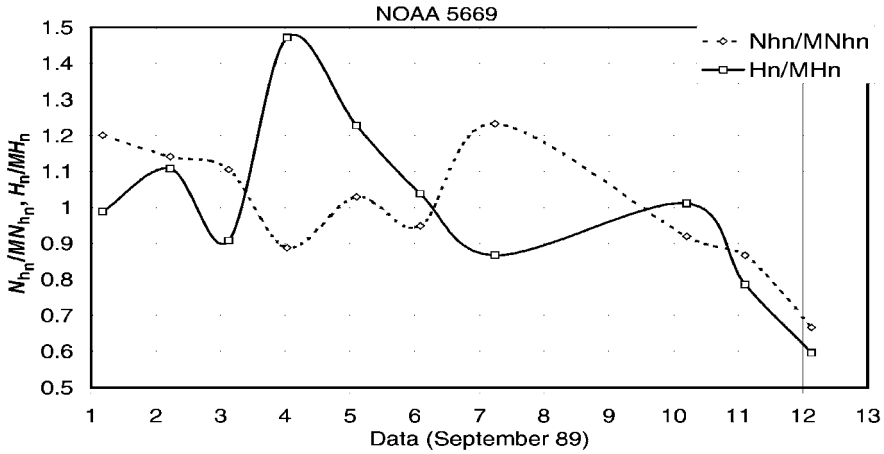


FIGURE 11 Time variations in the area N_{h_n} and flux H_n of the north polarity for NOAA 5669.

1989, in NOAA 5695 (see Figure 8). Such a relationship between the flux and area is possible when the flux increase is large.

In Figure 12 the logarithm of the daily average of the total length of the magnetic field inversion line for three large ARs (NOAA 5629, 5634 and 5643) is shown by open circles. These regions could be observed almost simultaneously from August 7 to August 22, 1989. Two curves in this plot show the logarithm of the daily average solar X-ray flux power ($W m^{-2}$) obtained from NOAA Bolder data; curves XL and XS are the upper and lower limits respectively. It can be seen that the correlation between these parameters is fair. The point for August 18, 1989, moved away from curve XS owing to neglect of data for some small ARs which were observed at this time and could contribute to the total X-ray flux.

Figure 13 shows the time variation in $F = E_{h_a} + E_{v_a}$ mentioned in Section 3.3. It is assumed that F had a sufficiently simple correlation between the derivative of the free energy of an AR area, with respect to $P = dF/dN_{h_a}$, and the pressure. Each point on the chart represents the daily average of the F parameter in NOAA 5395.

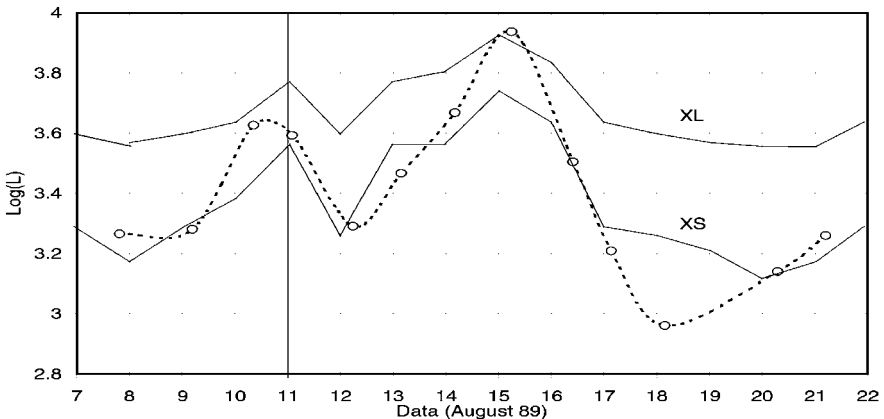


FIGURE 12 Logarithm of the total length of the inversion field line for three ARs in August 1989 (○) and X-ray fluxes (XL and XS values (—)).

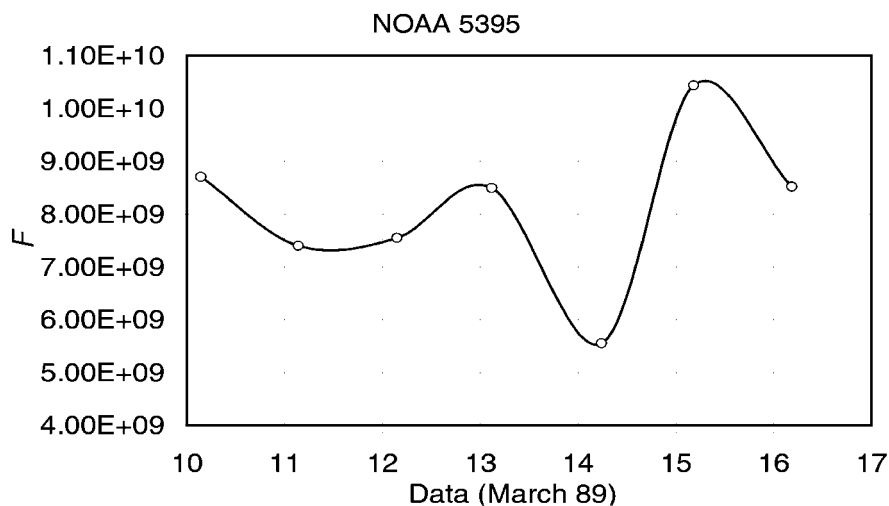


FIGURE 13 Time variation in the F parameter in NOAA 5395.

Figure 14 shows the time variation in P in the same AR (solid curve with open squares) and electron and proton time variations at the same time obtained from NOAA–NGDC Boulder data (<http://www.sel.noaa.gov/Data>). We can see that the correlation between these parameters could be obtained and the time changes in P correspond to the changes in particle fluxes.

7 SHORT-SCALE TIME VARIATIONS IN THE INTEGRAL PARAMETERS OF ACTIVE REGIONS

We can see that there are high correlations between the integral parameters of some ARs and X-ray fluxes; this is also true for data with an even better time resolution. So, for example in Figures 12–14, the time variations in the velocity flow in the AR NOAA 5395 for March 11 and 13, 1989, are given. The time series of observation data for these dates have sufficient

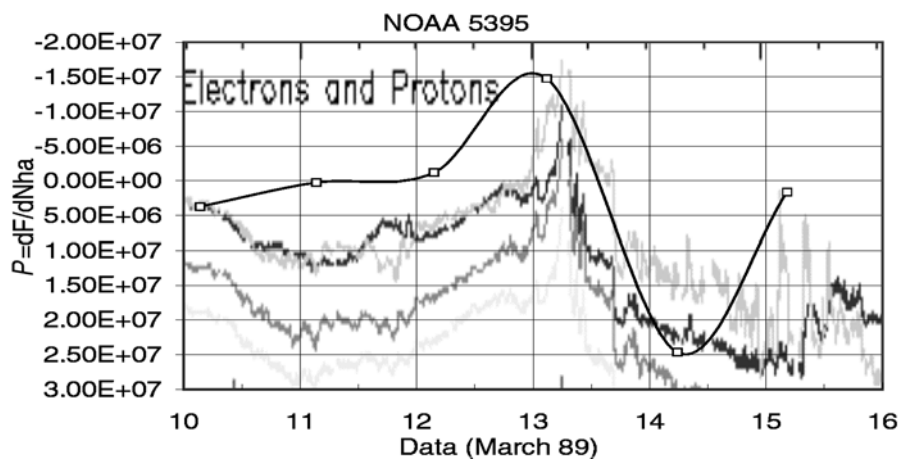


FIGURE 14 Time variations in P in NOAA 5395.

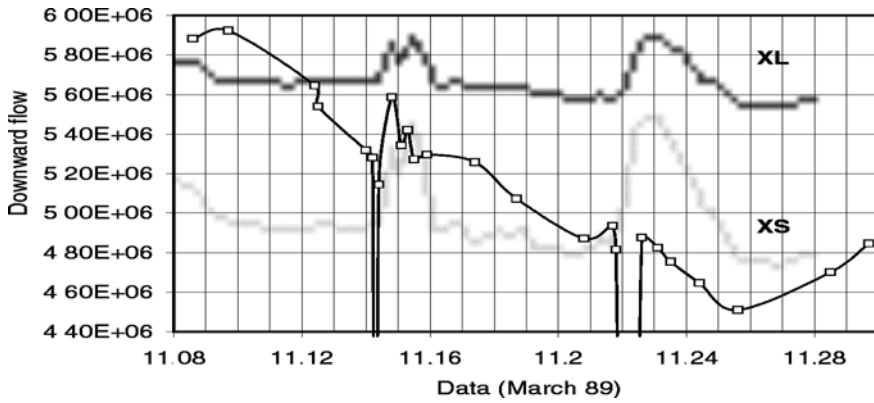


FIGURE 15 Red-shift flux and X-ray flares in NOAA 5395 (March 11, 1989).

time resolution for them to be compared with the 5 min average NOAA–NGDC Boulder data for X-ray fluxes (<http://www.sel.noaa.gov/Data>). During these dates there was only one superactive region on the Sun disc. A few other ARs were small and of low activity. So we can suppose that almost all X-ray flux was due to the superactive region.

Figures 15 and 16 show the time variations in the red-shift and blue-shift fluxes respectively in the AR of NOAA 5395 for March 11, 1989. The curves without open symbols show 5 min averages of the logarithm of Sun X-ray power fluxes (W m^{-2}); curves XL and XS are the upper and lower limits respectively. The curves with open symbols correspond to velocity flow in the AR. In Figures 15–20 the time (x axis) is given in parts of days. At 11.145 and 11.220 days (Figure 15) we can see a sharp degradation in red-shift flow and a simultaneous sharp increase in the blue-shift flow. The corresponding points are very pronounced in the Figures. That is, at these moments, we can see the beginning of the X-ray flares at the $M = 2.0$ and $M = 2.3$ points correspondingly. The maximum values of the X-ray flux were observed with some delay (about 10–15 min) after velocity bursts. Similar situations can also be seen in the figures for March 13, 1989 (Figures 17 and 18). From these two last figures one can see that the X-ray flare with $X = 1.2$ (see the date interval

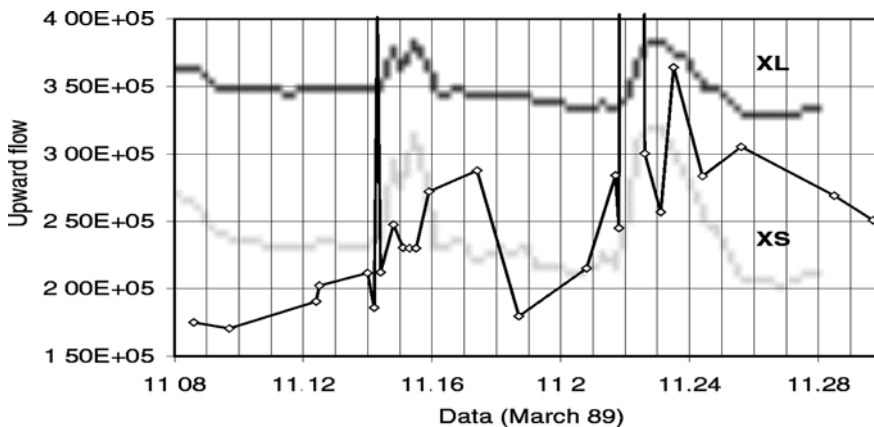


FIGURE 16 Blue-shift flux and X-ray flares in the same AR and in the same times.

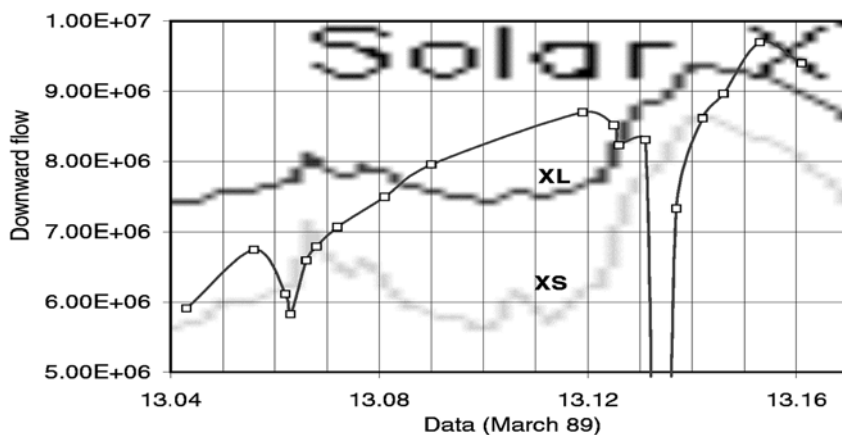


FIGURE 17 Red-shift flow and X-ray flares in the same AR on March 13, 1989.

from 13.12 days to 13.17 days) was preceded by a sharp increase in the blue-shift flow and a sharp decrease in the red-shift flow. The time delay in the X-ray flow maximum relative to the maximum value of the velocity flow was about 15 min, as in the previous cases. Not only do the velocity time variations have a close correlation with X-ray flares but also we discovered that time variations and other parameters that can be obtained from velocity maps show good correlations with X-ray flares. So we can state definitely that the velocity field pattern was sharply changed before the X-ray flow increases and further during all the time of the X-ray flare.

Figure 19 shows time variations in the structure parameter X (curve with open diamonds) and X-ray flux variations. The structure parameter X was specified by Chumak (1992). We can see from this figure that the fast and considerable changes in the velocity field structure preceded and followed X-ray flares.

Figure 21 shows time variations in the line velocity inversion length and time variations in the X-ray flux. We can see from this figure that X-ray flares preceded and followed essential variations in the field velocity inversion line length.

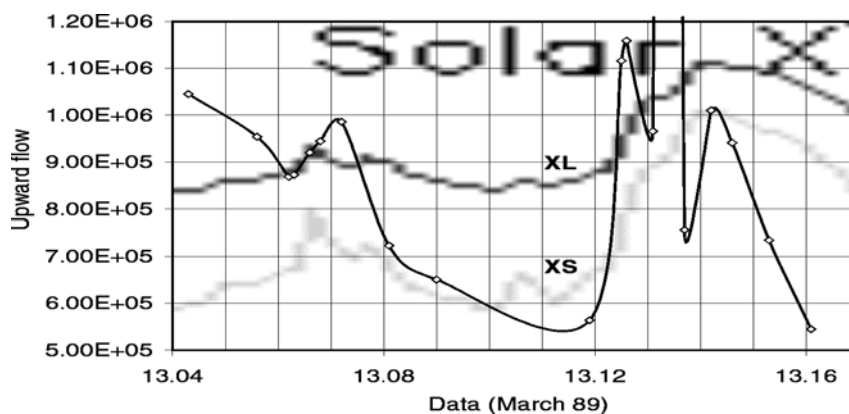


FIGURE 18 Blue-shift flux and X-ray flares in NOAA 5395 on March 13, 1989.

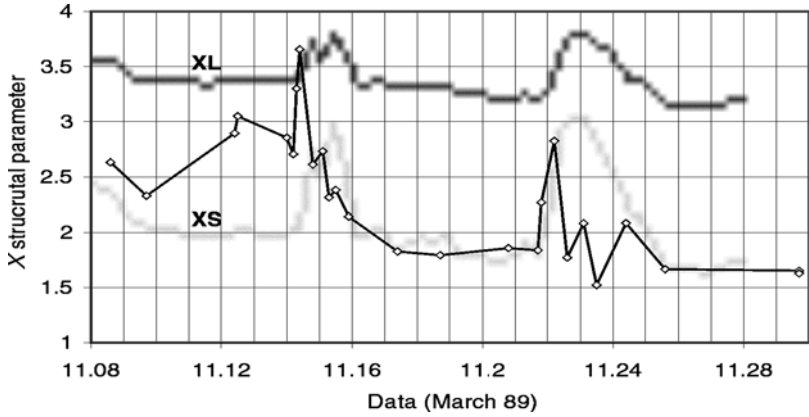


FIGURE 19 Time variations in the structure parameter X during the time of X-ray flares in NOAA 5395 on March 11, 1989.

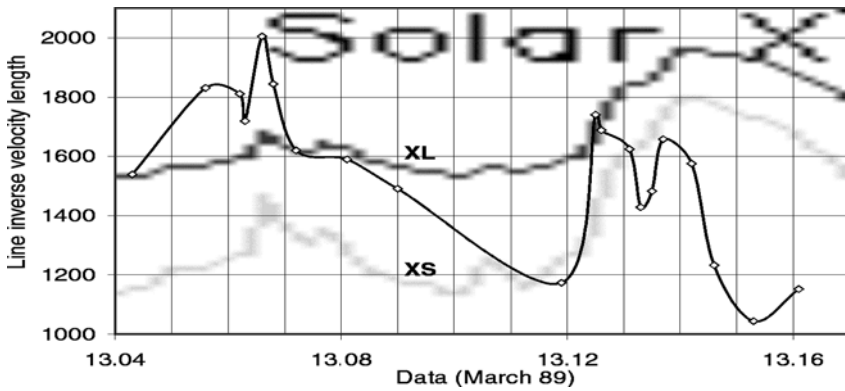


FIGURE 20 Time variations in the length of the velocity field inversion line during the time of X-ray flares in NOAA 5395 on March 13, 1989.

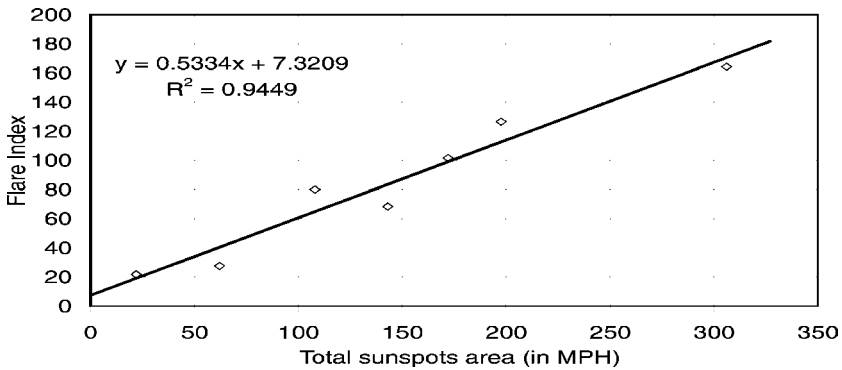


FIGURE 21 Correlation between the sunspot area (in MPHs) and flare index for seven ARs.

8 SOME BINARY CORRELATIONS OF INTEGRAL PARAMETERS; PROBLEM OF NUMERICAL IDENTIFICATION OF THE CURRENT STATES OF ACTIVE REGIONS

The time variations that we considered in the last section give us important information about individual peculiarities of ARs. This information can be interesting from a practical point of view, for forecasting geomagnetic events for instance. However, from the viewpoint of physical theory of solar ARs the correlations between various integral parameters, which are independent of time, seem to be more important. Let us consider initially two such invariant correlations for example.

Figure 21 shows the correlation between the daily average flare index and the daily average sunspot area for seven ARs. This figure provides in another form the data that we have examined in Figure 4. From Figure 21 we can see a good linear correlation between these parameters (reliability of the approximation, $R^2 = 0.945$).

Figure 22 shows us a sufficiently high correlation of the flare index with the daily average magnetic field gradient calculated along the inversion line for NOAA 5629.

We can give more examples of good correlations between the flare index and some parameters of the magnetic field or velocity field in solar ARs. For instance in the paper by Bao *et al.* (1999) a temporal relationship between chromosphere H_β flares and photosphere current helicities in ARs has been obtained. These examples are sufficient to illustrate the idea that flare activity in an AR depends on their current status and that the number of AR integral parameters shows strong correlations with the relative flare index.

So we can consider some of our AR integral parameters as the AR state parameters. From the theory point of view, binary correlations of such state parameters are of specific interest. For example Figure 23 shows the correlation between two such state parameters for the AR NOAA 5395; namely the above-mentioned parameters P and N_{h_a} . If we suppose that the volume of the AR differs from the area N_{h_a} by some constant multiplier factor, then we can regard the correlation shown in Figure 23 as the analogue of the familiar thermodynamic (P, V) diagram.

The next example is given in Figure 24. In this figure the correlation between the Shannon entropy and total magnetic flux area for the AR NOAA 5629 is shown. We can regard this correlation also from a thermodynamics point of view.

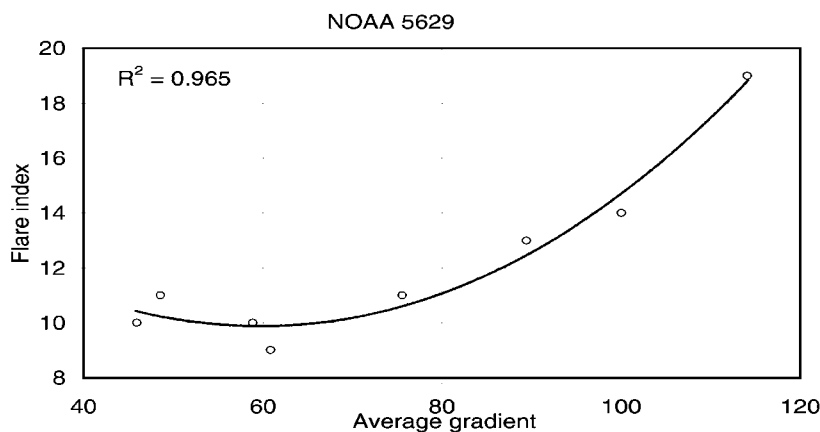


FIGURE 22 Correlation between the flare index and the average (along the inversion line) gradient of the magnetic field (in gauss per discrete area).

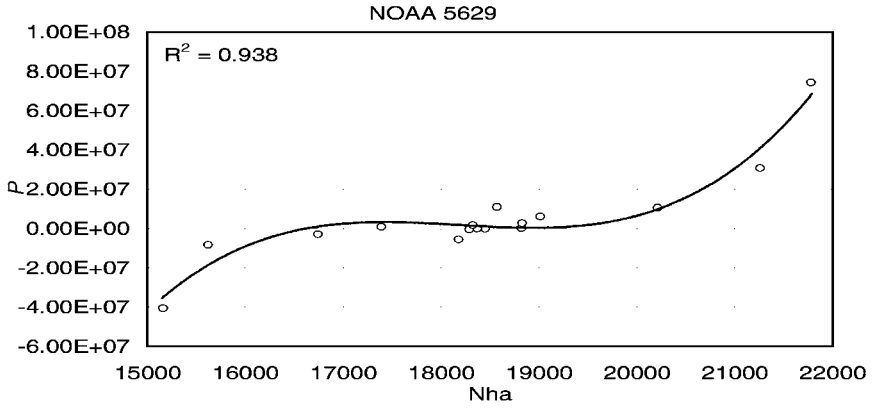


FIGURE 23 Correlation between P and the area for the AR NOAA 5629.

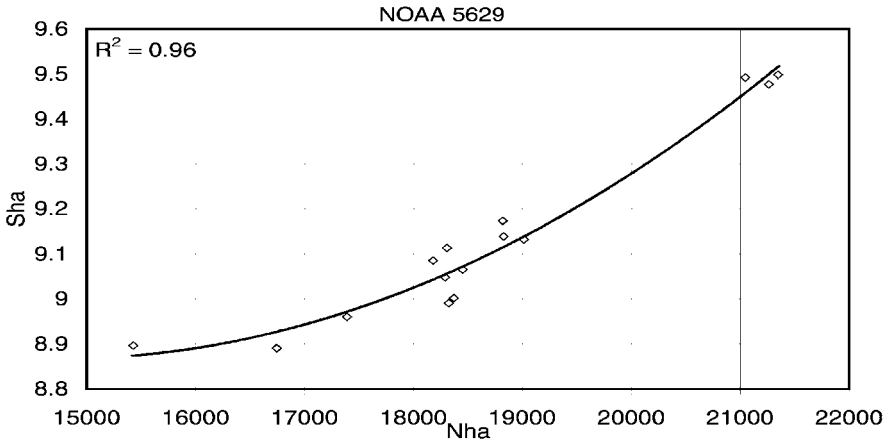


FIGURE 24 Correlation between the entropy and the magnetic flux area for the AR NOAA 5629.

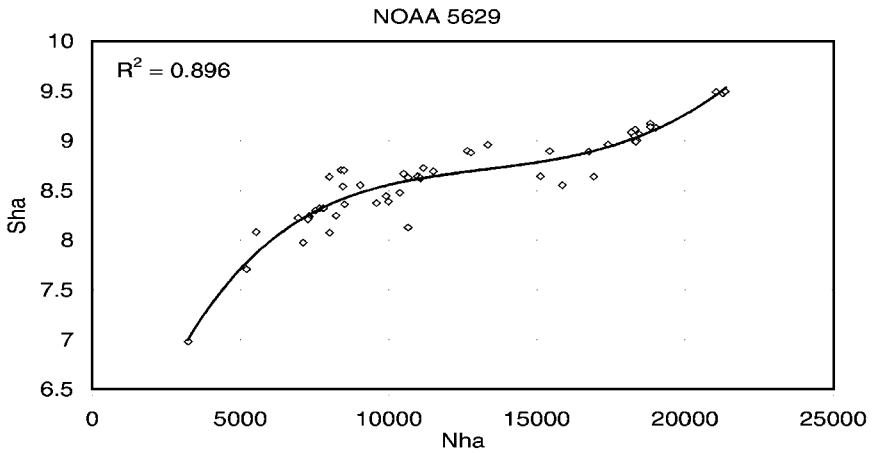


FIGURE 25 Correlation between the entropy and the magnetic flux area for NOAA 5629.

The last correlation of this kind is given in Figure 25. Here one can see the correlation between the Shannon entropy and magnetic flux area for all ten ARs. This correlation is also of some interest for the thermodynamics of ARs. We can see from Figure 25 that ARs have different positions on the plot. So a comparison of Figures 24 and 25 shows that an extension of the AR NOAA 5629 has been located in the top right corner of the plot during the total AR observation time.

9 DISCUSSION

In this paper we analyse the problem of obtaining the minimum number of quantitative parameters, which are necessary and sufficient for unique identification of the current state of an AR. It is possible to propose many such parameters as can be seen. The problem is to select from this large quantity of parameters the minimum number of necessary and sufficient for our purposes. In principle we could obtain a solution of the problem with the help of a physical model of the AR if such a model exists. As is known, there are no strong physical models of an AR. There are only a few reliable scenarios, which ambiguously interpret the origin and development of this magnetohydrodynamic structures. Uncertainties in the theory do not allow us to solve our problem uniquely.

Conventionally one can consider all magnetoplasma models on three levels: thermodynamic or virial level; that is a simple model giving a very overall and averaged description; magnetohydrodynamic level, that is a more complete model giving a more detailed picture of the dynamics of magnetic and velocity fluxes; kinetic level corresponding to a very complete and detailed model. One can see a good interrelation between theory and observations when the detailed theory corresponds to accuracy of observations.

So kinetic models are good for understanding the physical processes in interplanetary plasma and solar corona. Magnetohydrodynamic models of physical processes and magnetoplasma structures above the photospheric level and many highly accurate observations agree well now and, as a result, we can see an advanced understanding of physical processes in this region.

On the contrary, we have very poor information about the regions lying under the photospheric level, and it is these levels that produce the ARs and control their dynamics and development. We can draw conclusions about the physical state and physical processes in subphotospheric layers only from observation of the photosphere level and from a few helioseismological results. So we have only a few direct and accurate observations of these layers. Under these conditions, one can propose using magnetohydrodynamic theory many essentially different scenarios that do not contradict all these observational data. Therefore the quantity and quality of these observational data for subphotosphere layers are not sufficient to construct a strong and single-valued magnetohydrodynamic model for ARs.

It is quite possible that a less detailed and more widely applicable model of thermodynamic type could be better than the more challenging models under these conditions. As long as the subphotosphere plasma is an inhomogeneous and non-equilibrium medium, then we can discuss ARs in terms of non-equilibrium structure theory, and non-equilibrium thermodynamics can be regarded as a meta-theory, suitable for the design of AR models. Such models of ARs can be based on common physical techniques such as conservation laws, virial proportions and scaling evaluation. In such an approach some invariant proportions between integral parameters of an AR can be interpreted as dependences between thermodynamic state functions. The determination and examination of such dependences can allow us theoretically to find the state equations and to construct the closed phenom-

ological theory of ARs completely, based on observational data. Such a closed theory can in a natural way solve the problem concerning the number of parameters necessary and sufficient for unique identification of the current states of the AR. So the non-equilibrium thermodynamics of solar ARs can be constructed by extracting from observational data the extensive and intensive parameters having a thermodynamic sense. We considered some of these parameters in this paper. Such parameters as the magnetic polarity areas, the red-shift and blue-shift region areas, the Shannon entropies of magnetic and velocity fluxes, the total magnetic fluxes of different magnetic polarities, the total velocity fluxes in the red- and blue-shift regions and the total energies of the magnetic field and velocity field are extensive parameters. Examples of intensive parameters are the average magnetic fields of different polarities, the average red and blue shifts and the parameter P can analogue of pressure. It should be noted that a few nondimensional intensive parameters define the 'disbalance' of extensive parameters and thus quantitatively characterize the level of openness of an AR as a thermodynamic system.

The invariant correlation between the parameters (see Figures 23–5, for instance) can be regarded as a basis for searching for the state equation for ARs as thermodynamic systems. This state equation could be based only on observational data and so it could be a good basis for theoretical developments in the construction of AR models as open thermodynamic systems.

However, we should note a few peculiar properties of solar ARs as thermodynamic systems. The first is the high degree of their openness. For some of these ARs the 'disbalance' of the indices reaches large values. In the light of this fact the current states of these systems can be very dependent on external conditions. One such condition could be the hydrodynamic situation in the region where an AR arises and develops. As can be seen from the observations, the motion of the magnetic flux tubes is very complicated sometimes and its statistical parameters can be very different for different ARs. As a result, a situation is possible where ARs with nearly the same total magnetic fluxes can demonstrate essential differences in activity levels. It has been shown (Chumak *et al.*, 1987) that two parameters mentioned above, namely distance between the polarity centres in an AR and the corner between the magnetic axis of the AR and the local parallel, in most cases are sufficient to describe the kinematic peculiarities of ARs. The number of correlations between these parameters and other properties of ARs have been discussed by Tian *et al.* (1999).

The second feature of solar ARs as thermodynamic systems is the presence of some extensive and intensive parameters of non-thermodynamic type but very effective for describing the current state of ARs. They include the following parameters: the length of the magnetic field inversion line, the length of the velocity inversion line, the maximal and average gradients along the inversion lines mentioned in this paper, and the current helicity discussed by Bao *et al.* (1999). The mutual relations between these parameters and parameters of thermodynamic type are vague at the present time.

There are questions also about some thermodynamic parameters, which should be clarified, for example whether our parameter F represents the free active region energy sufficiently well. Another question is whether the informational entropy mentioned in this paper has a thermodynamic sense or not. Now we can assert that it has (Ebeling, 1976; Klimontovch, 1987, 1990). However, it is clear that statistical and canonical distributions should correspond to the system, which creates the considered structures and for which free energy and entropy are determined as state functions. If, as in our case, these functions are magnetic fluxes, then it should be the statistics and distributions of those magnetoplasma elements from which these magnetic fluxes were constructed.

We discussed above the high correlation between the total magnetic fluxes and the total red-shift fluxes in the ARs. This observational result has been discussed in a number of

papers (see for example Bonacini *et al.* (1989)). It is a very interesting problem. The fact that an AR boundary depends on the method of observation and even the concept of boundary is very relative. An AR in white light is a sunspot group. In that case we have a multilinked area equal to the total sunspot area. In magnetometric observational data for the same AR we can see that the region with a magnetic field greater than the background value has an essentially larger size than the total sunspot area. Observing the ‘disbalance’ index for velocity fields (-0.8 , i.e. the red-shift flux is 80% of the total flux) means that the hydrodynamic flux space associated with an AR is larger than magnetic flux space. So we can assume that either ARs as dynamic systems are more extensive objects than the corresponding sunspot groups and magnetic fluxes, or that ARs arise in downward flow regions. In both cases the problem of coordination of that observational fact with the scenario of magnetic flux tubes floating to the surface (Parker, 1958, 1979) does not have a good solution at present.

From a practical point of view there are interesting results on the correlations of various AR integral parameters with particles and X-ray flow variations (see Figures 12–20). These results could be used for space weather forecasting.

From a theory point of view there is the interesting fact that changes in the total sunspot areas and total magnetic fluxes in some ARs have an irregular character (see Figures 7–9). This effect is associated with the magnetic θ pinch well known in plasma physics; this occurs where an increase in magnetic flux in the magnetic flux tube correlates with a reduction in its cross-sectional area. Plasma ejection from the magnetic flux tube is one of the corollary fact of this effect. Something similar may take place in solar ARs from time to time.

The main result of this paper from our point of view consists of the fact that investigation of time variations and mutual correlations of the AR integral parameters is very promising from both theoretical and practical points of view. We hope to offer the results of examinations of some special questions from this field in subsequent papers.

Acknowledgements

The authors would like to thank the staff of Huairou Solar Observing Station of National Astronomical Observatories of China for the magnetogram observations. This study is supported by Chinese Academy of Sciences and National Natural Scientific Foundation of China.

References

- Allen, C.W. (1973). *Astrophysical Quantities*, Athlone Press, London.
- Bao, S.D., Zhang, H.Q., Ai, G., and Zhang, M. (1999). *Astron. Astrophys. Suppl.*, **139**, 311.
- Bishop, C.M. (1995). *Neural Networks and Pattern Recognition*, Oxford University Press, Oxford.
- Bonacini, D., Degl’Innocenti, E.L., November, L.J., and Smaldone, L.A. (1989). *High resolution spectrophotometry of an active region*, UAI Symposium Vol. 138, Kiev, Naukova Dumka, p. 181.
- Chumak, O.V. (1992). *Physics of the Solar Atmosphere*, Gilim, Alma-Ata, p. 65 (in Russian).
- Chumak, O.V., and Chumak, Z.N. (1987). *Kinematics and Physics of Heavenly Bodies*, Vol. 3, Part 3, p. 7 Kiev, Naukova Dumka (in Russian).
- Chumak, O.V., Chumak, Z.N., and Minosiants, G.S. (1987). *Solnechnye Dannye*, **10**, 63.
- Ebeling, W. (1976). *Strukturbuilding bei irreversiblen Prozessen*, Teubner.
- Gilmore, R. (1981). *Catastrophe Theory for Scientists and Engineers*, Wiley, New York.
- Klimontovich, Yu.L. (1987). *Physica A* **142**, 390.
- Klimontovich, Yu.L. (1990). *Turbulent Motion and Structure of Chaos*, Nauka, Moscow.
- Landau, L.D., and Lifshits, E.M. (1976). *Statistical Physics*, Part 1, Nauka, Moscow.
- Murray, A.F. (1995). *Applications of Neural Nets*, Kluwer, Dordrecht.
- Parker, E.N. (1958). *Astrophys. J.* **128**, 664.
- Parker, E.N. (1979). *Cosmic Magnetic Fields*, Oxford University Press, Oxford.
- Tian, L., Zhang, H., Tong, Y., and Jing, H. (1999). *Solar Phys.* **189**, 305.
- Veselovsky, I. (1999). Report SMR11-61/10, International Center for Theoretical Physics, Trieste, Italy.
- Wang, H., Denker, C., Spirook, T., Goodi, P.R., Yang, S., Marquette, W., Varsik, J., Fear, R.J., Nenow, J., and Dingley, D.D. (1998). *Solar Phys.* **183**, 1.